

Supporting Information

Pt nanoparticles supported on $\text{YCo}_x\text{Fe}_{1-x}\text{O}_3$ perovskite oxides: Highly efficient catalysts for liquid-phase hydrogenation of cinnamaldehyde

Yujie Xue,^a Huiyue Xin,^a Wenhui Xie,^b Peng Wu^a and Xiaohong Li,^{a,*}

^a *Shanghai Key Laboratory of Green Chemistry and Chemical Processes, School of Chemistry and Molecular Engineering, East China Normal University, 3663 North Zhongshan Rd., Shanghai 200062, China. E-mail: xhli@chem.ecnu.edu.cn*

^b *School of Physics and Materials, East China Normal University, 3663 North Zhongshan Rd., Shanghai 200062, China*

Contents

Experimental

1. Preparation of Pt/YCo _x Fe _{1-x} O ₃ catalyst	3
2. Characterization	4
3. Catalytic test.....	5
Fig. S1 Wide-angle XRD patterns of the Pt-based catalysts and YCo _x Fe _{1-x} O ₃ supports.....	6
Fig. S2. N ₂ -physisorption isotherms of Pt/YCo _x Fe _{1-x} O ₃ catalysts	7
Fig. S3. SEM images of (a, b) YCoO ₃ ; (c, d) YCo _{0.3} Fe _{0.7} O ₃ ; (e, f) Pt/YCo _{0.3} Fe _{0.7} O ₃ -fresh and (g, h) Pt/YCo _{0.3} Fe _{0.7} O ₃ -used	8
Fig. S4. The correlation of Mass Specific Rate versus the molar ratio of Co/Fe	9
Fig. S5. TEM images and Pt particle size distribution of the used Pt/YCo _{0.3} Fe _{0.7} O ₃ catalyst.....	10
Fig. S6. TG curve of the used Pt/YCo _{0.3} Fe _{0.7} O ₃ catalyst	11
Table S1. Comparison of the Pt-based catalysts for the selective hydrogenation of CAL to yield COL.	12
Fig. S7. HAADF-STEM images and STEM-EDS elemental mapping images for the area enclosed by the orange square for Pt/YCoO ₃ ; Pt/YFeO ₃ and Pt/YCo _{0.3} Fe _{0.7} O ₃	13
Fig. S8. XPS spectra of the Pt/YCo _x Fe _{1-x} O ₃ catalyst.....	15
Fig. S9. The correlation of COL selectivity versus Pt ⁰ amount on the Pt/YCo _x Fe _{1-x} O ₃ catalyst according to XPS result	16

Experimental

1. Preparation of Pt/YCo_xFe_{1-x}O₃ catalyst

SBA-15 was synthesized using the triblock copolymer Pluronic 123 and tetraethyl orthosilicate (TEOS) according to Ref. [1]. YCo_xFe_{1-x}O₃ perovskite-type composites were prepared by a modified sol-gel method [2]. The starting materials Y(NO₃)₃·6H₂O, Co(NO₃)₂·6H₂O, and Fe(NO₃)₃·9H₂O were dissolved in distilled water with a stoichiometric ratio of Y/Co/Fe=1/1/0, 1/0.7/0.3, 1/0.5/0.5, 1/0.3/0.7; 1/0/1, respectively. Citric acid was added to the above nitrate solution as a complexing agent to control the final citrate/transition metal ratio of 1/1. Then, SBA-15 (1.0 g) after sonicated in 10 mL deionized water was introduced to the above mixture. Subsequently, the solution was stirred for 3-4 h at room temperature. Next, the mixed solution was moved to a water bath at 90 °C until the sticky gel was formed. After that, the gel was dried at 140 °C overnight. After grinding, the precursor was calcined at 500 °C with a ramping rate of 5 °C/min and kept at 500 °C for 4 h, followed by further calcination at 950 °C with a ramping rate of 3.5 °C/min and remained at 950 °C for 5 h. Finally, the resultant powders were treated with sodium hydroxide solution (2 mol/L) to remove the SBA-15 template.

The nominal 5 wt% Pt catalysts were prepared via an impregnation method using an aqueous solution of H₂PtCl₆. The suspension was stirred for 4-6 h at room temperature and then evaporated to remove the excess solvent, followed by drying overnight at 100 °C. Finally, catalyst precursors were reduced in an aqueous solution of sodium formate at 90 °C after calcined in air at 200 °C for 2 h.

References

- [1] D. Zhao, J. Feng, Q. Huo, N. Melosh, G. H. Fredrickson, B. F. Chmelka, G. D. Stucky, *Science*, 1998, 279, 548-552.
- [2] Y. Wei, H. Gui, Z. Zhao, J. Li, Y. Liu, S. Xin, X. Li, W. Xie, *AIP Adv.*, 2014, **4**, ID: 127134.

2. Characterization

Powder X-ray diffraction (XRD) patterns of the samples were collected on a Bruker D8 ADVANCE instrument using Cu K α radiation ($\lambda=1.54178$ Å) as X-ray source. The N₂-physisorption isotherms of samples were measured at 77 K on a Quantachrome Autosorb-3B system after the samples were evacuated at 300 °C for 4 h. The Brunauer-Emmett-Teller (BET) specific surface area was calculated using adsorption data in the relative pressure range from 0.05 to 0.35. Scanning electron microscopy (SEM) was performed using a Hitachi S-4800 microscope. The transmission electron microscopy (TEM) images were taken on an FEI Tecnai G2-TF30 microscope at an acceleration voltage of 300 kV. The actual Pt loading of samples was determined by Thermo Elemental IRIS Intrepid II XSP inductively coupled plasma-optical emission spectroscopy (ICP-OES). The thermogravimetric (TG) analysis of the samples was conducted from r.t. to 800 °C under an air atmosphere with Mettler Toledo TGA/SDTA851^e apparatus.

X-ray photoelectron spectrum (XPS) of the samples were measured with a Thermo Fisher Scientific ESCALAB 250Xi spectrometer with Al K α radiation (1486.6 eV) as incident beam with a monochromator. The samples were directly measured only after pretreatment under vacuum. The binding energy (BE) was calibrated using C-C binding energy at 284.4 eV in order to compare the BEs with the data from the literature. The spectra shown in the figures have been corrected by subtraction of a Shirley background. Spectral fitting and peak integration was done using the XPSPEAK software.

Temperature-programmed reduction with hydrogen (H₂-TPR) was conducted to understand the interaction between Pt and support with a Micromeritics AutoChem II Chemisorption Analyzer. Prior to H₂-TPR experiments, the samples were pretreated in flowing Ar at 300 °C for 1 h and then cooled to room temperature in flowing Ar (99.999%, 50 mL/min).

After that, the sample was heated from room temperature to 800 °C with a heating rate of 10 °C/min under a mixture of 10% H₂-Ar (50 mL/min). The rate of H₂ consumption was monitored by a gas chromatograph (GC) with a thermal conductivity detector (TCD).

3. Catalytic tests

A certain amount of catalyst was pretreated under hydrogen atmosphere (99.999%, 30 mL/min) at 200 °C for 2 h before use. The catalyst was then mixed with solvent and CAL without further exposure to air, which was subsequently transferred to a 100-mL autoclave. The hydrogenation reaction began with stirring (1000 rpm) at a designated temperature after hydrogen (2.0 MPa) was introduced into the autoclave. The reaction was stopped after a proper time, and then the products were analyzed by GC-FID (GC-2014, Shimadzu Co.) equipped with a capillary column (DM-WAX, 30 m × 0.25 mm × 0.25 μm).

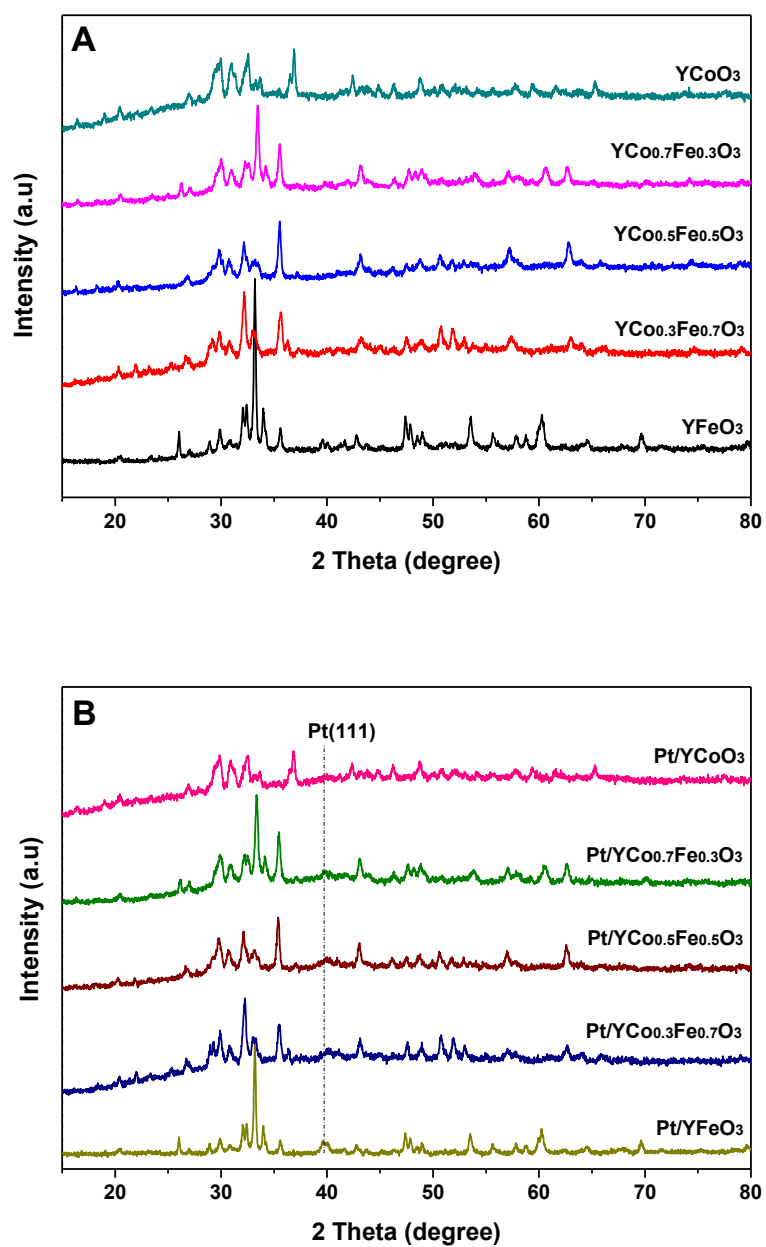


Fig. S1. Wide-angle XRD patterns of the Pt-based catalysts and YCo_xFe_{1-x}O₃ supports.

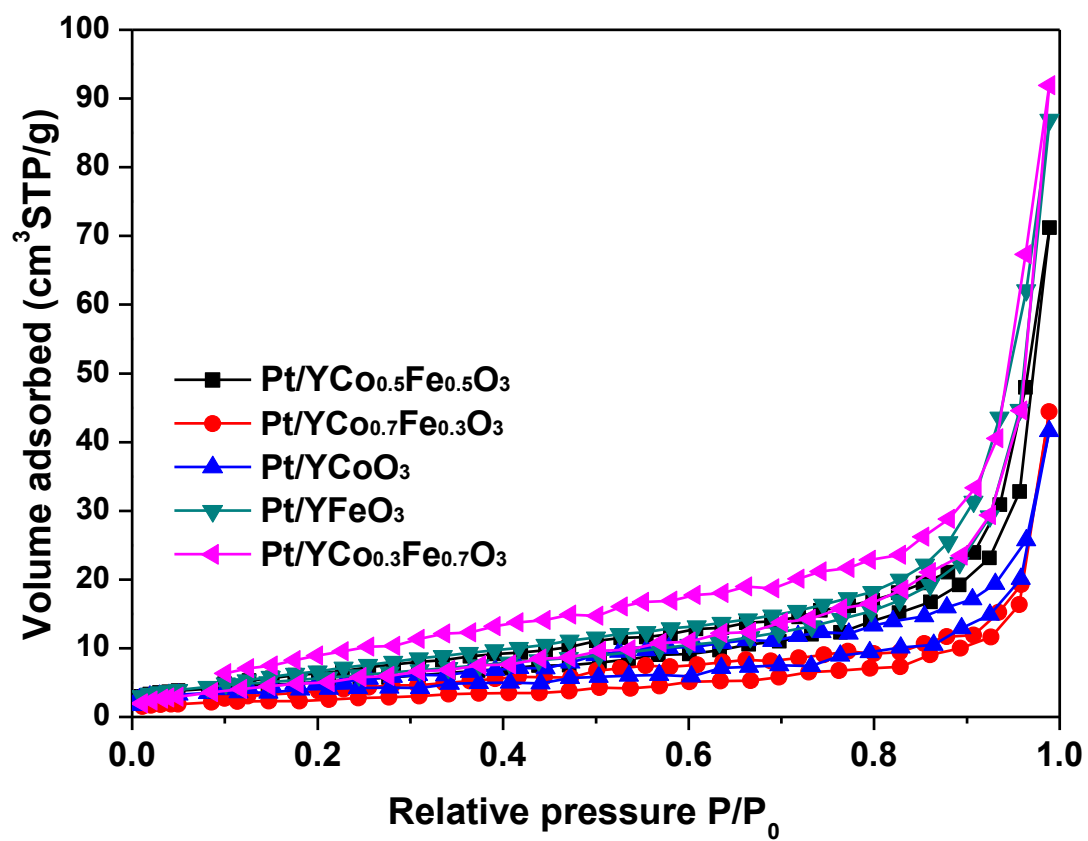


Fig. S2. N₂-physorption isotherms of Pt/YCo_xFe_{1-x}O₃ catalysts.

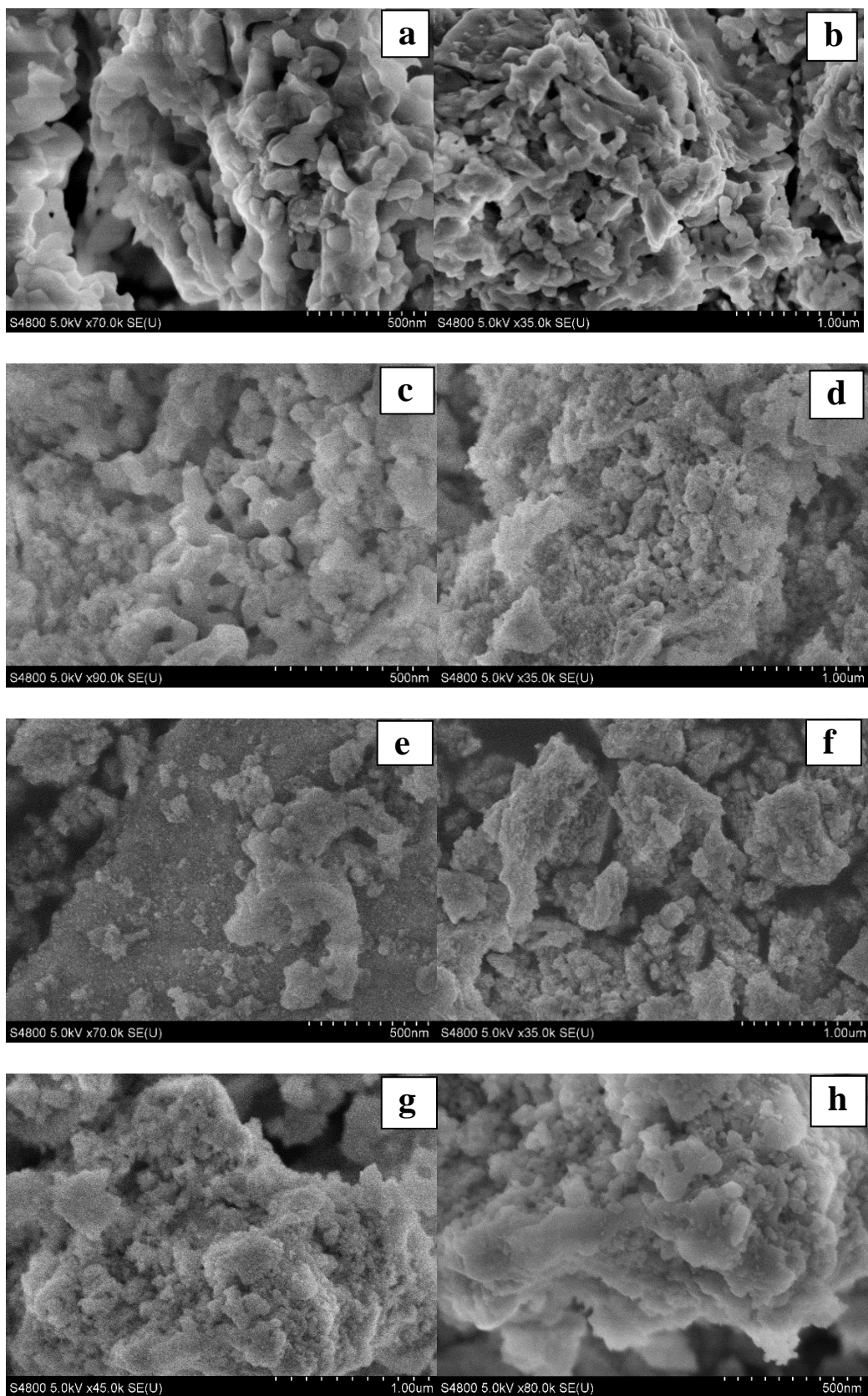


Fig. S3. SEM images of (a, b) YCoO_3 ; (c, d) $\text{YCo}_0.3\text{Fe}_0.7\text{O}_3$; (e, f) $\text{Pt}/\text{YCo}_0.3\text{Fe}_0.7\text{O}_3$ -fresh and (g, h) $\text{Pt}/\text{YCo}_0.3\text{Fe}_0.7\text{O}_3$ -used.

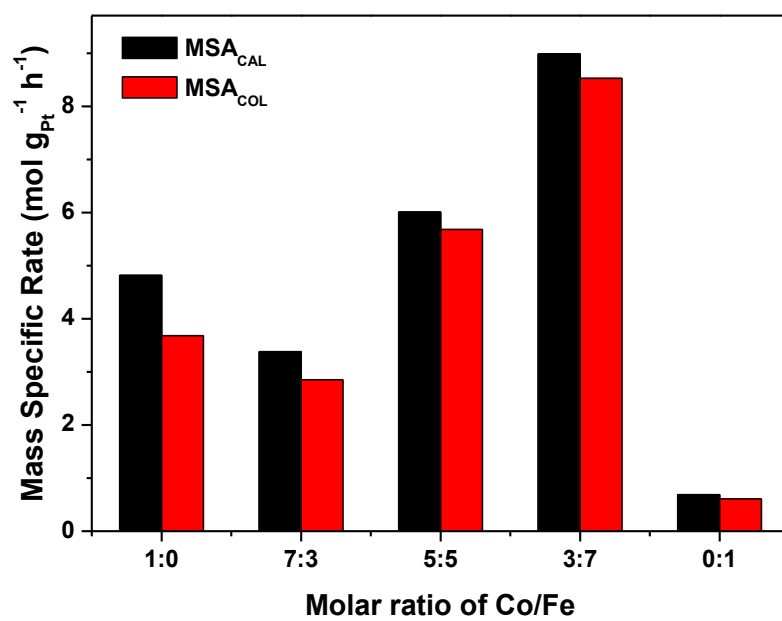


Fig. S4. The correlation of Mass Specific Rate versus the molar ratio of Co/Fe.

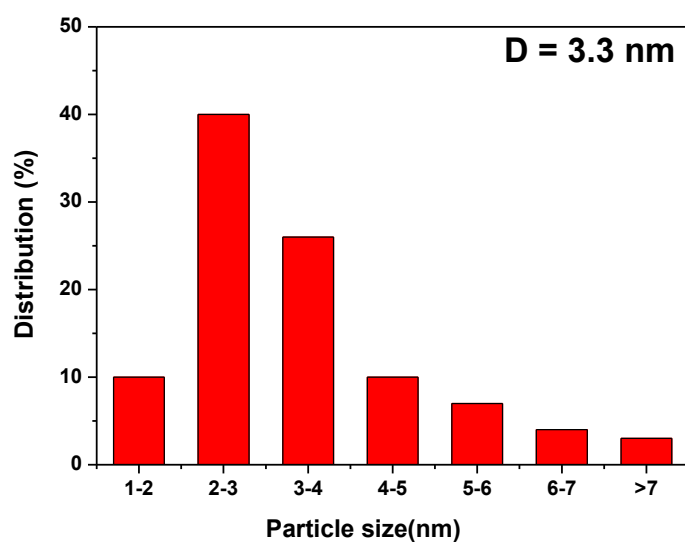
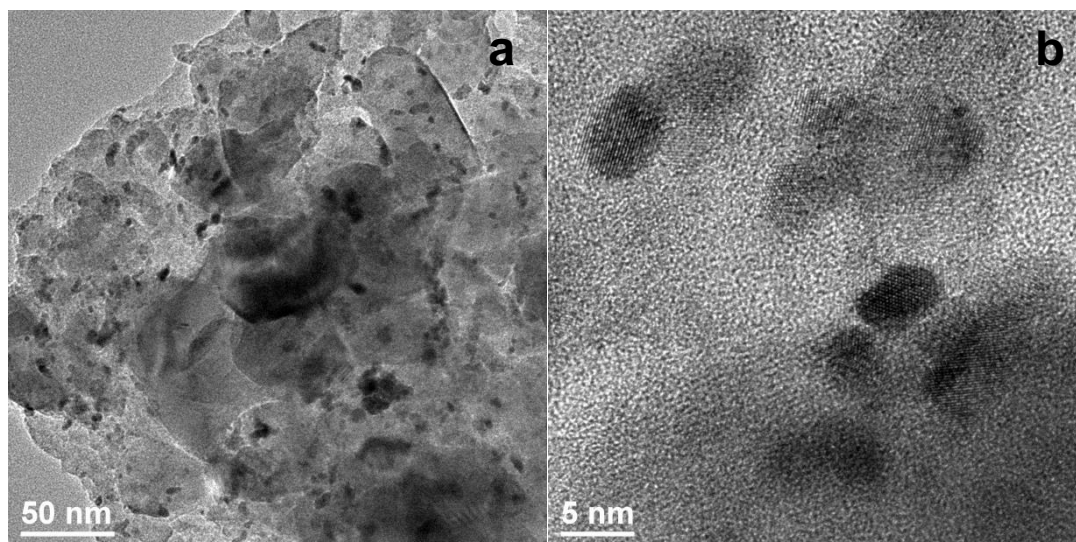


Fig. S5. TEM images and Pt particle size distribution of the used Pt/YCo_{0.3}Fe_{0.7}O₃ catalyst.

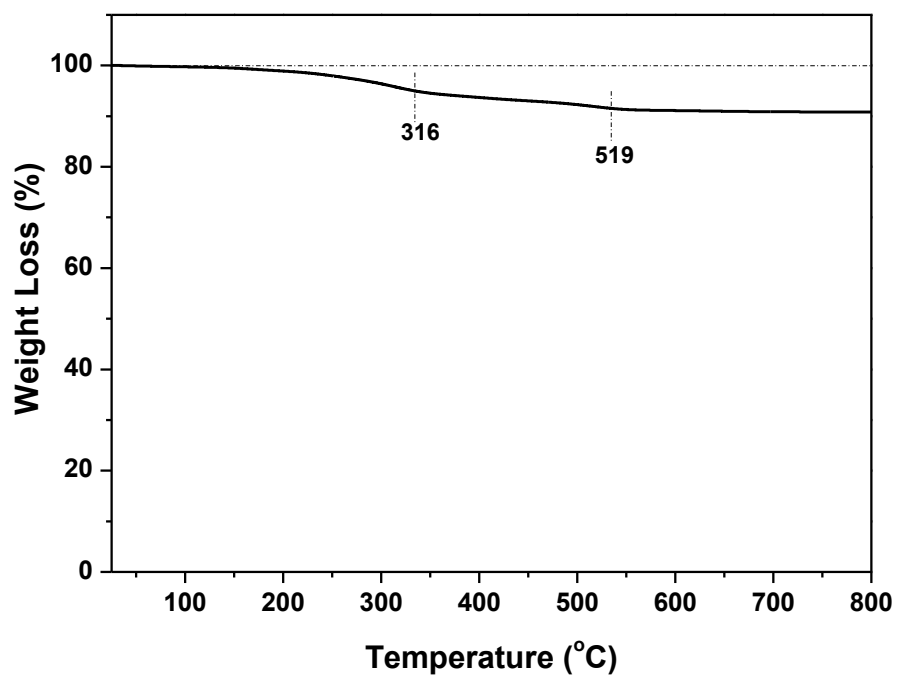


Fig. S6. TG curve of the used Pt/YCo_{0.3}Fe_{0.7}O₃ catalyst.

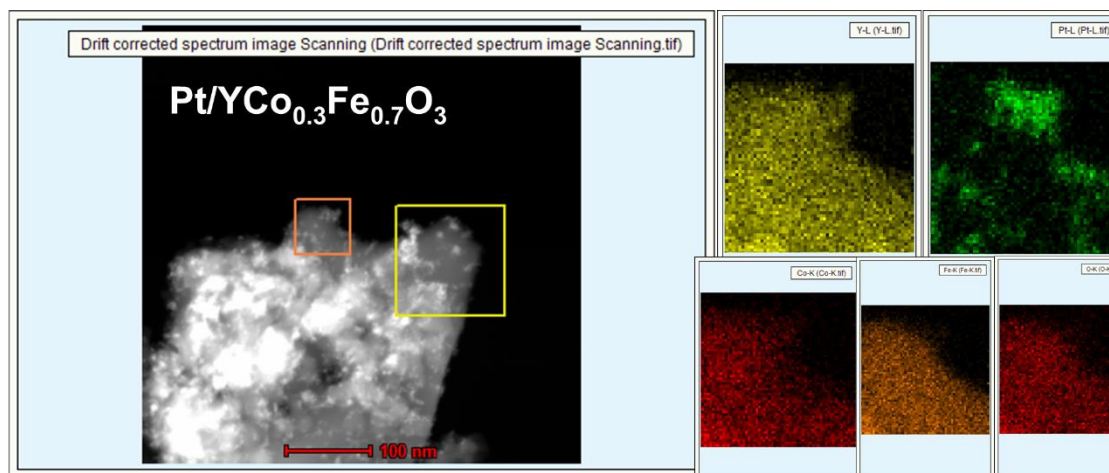
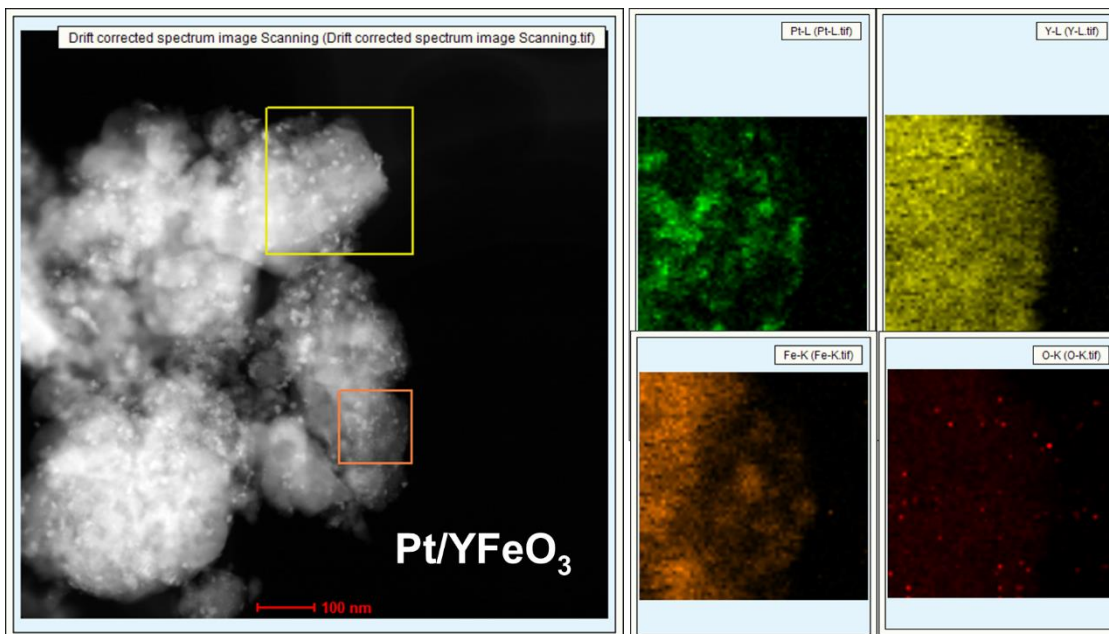
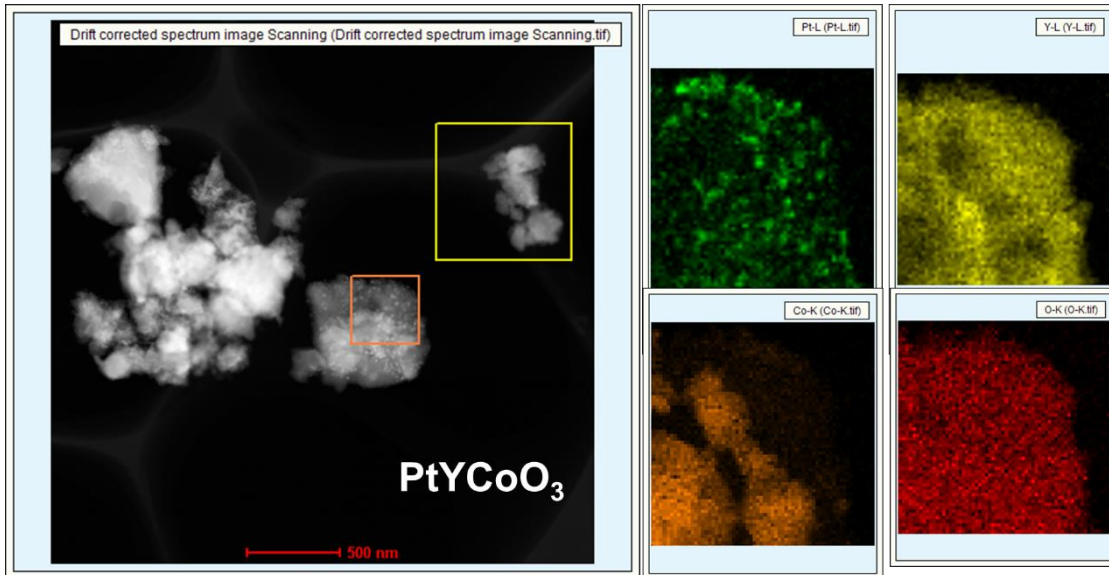
Table S1. Comparison of the Pt-based catalysts for the selective hydrogenation of CAL to yield COL.

Catalyst	T (°C)	P _{H₂} (MPa)	t (h)	Conv. (%)	COL Sel. (%)	TOF (h ⁻¹)	MSR ^a (mol/(g·h))	Ref.
Pt-1a/n-Al ₂ O ₃	30	1.0	3	99.0	91.0	3746	-	3
PtFe _{0.25} /15AS	90	2.0	1	77.4	76.9	5544	13.9	5
PtFe _{0.25} /15TS	90	2.0	0.5	68.0	86.4	11016	12.2	6
Pt/SiC-C	25	2.0	1	84.9	80.0	2446	-	7
Pt/TiO ₂ -SiO ₂	80	4.0	0.5	98.8	91.0	-	3.9×10 ⁻²	8
Pt/CeZrO ₂ -1.5	60	1.0	0.5	95.0	94.0	10423	-	9
Pt/3DHPC	70	2.0	1	92.7	91.1	1554	-	10
Pt-Mo ₂ N/SBA-15	80	1.0	2	70.8	76.9	521	-	13
PtFe NWs	70	0.1	2.5	95.7	95.5	100	-	14
Pt ₃ Fe/CNT	60	2.0	0.5	62.1	97.2	1200	-	15
MIL-101@Pt@FeP-CMP ^{sponge}	RT	3.0	0.25	97.6	97.3	1516	-	19
Pt/FeFe-LDH	110	1.0	2	90.0	92.0	1026	-	21
Co-Pt/C-0.6	80	2.0	2	100	99.0	15084	-	24
Pt/YCo _{0.3} Fe _{0.7} O ₃	90	2.0	0.5	98.9	94.9	15163	31.1	This study

^a: MSR means mass-specific rate, defined as the converted CAL or formed COL per gram of Pt per hour

References:

- [3] H. Liu, Q. Mei, S. Li, Y. Yang, Y. Wang, H. Liu, L. Zheng, P. An, J. Zhang, B. Han, *Chem. Commun.*, 2018, 54, 908.
- [5] H. Pan, J. Li, J. Lu, G. Wang, W. Xie, P. Wu, X. Li, *J. Catal.*, 2017, 354, 24-36.
- [6] Y. Xue, R. Yao, J. Li, G. Wang, P. Wu, X. Li, *Catal. Sci. Technol.*, 2017, 7, 6112-6123.
- [7] R. Yao, *RSC Adv.*, 2016, 6,
- [8] Q. Wu, C. Zhang, B. Zhang, X. Li, Z. Ying, T. Liu, W. Lin, Y. Yu, H. Cheng, F. Zhao, *J. Colloid Interf. Sci.*, 2016, 463, 75-82.
- [9] S. Wei, Y. Zhao, G. Fan, L. Yang, Li, F. Li, *Chem. Eng. J.*, 2017, 322, 234-245.
- [10] D. Hu, W. Fan, Z. Liu, L. Li, *ChemCatChem*, 2018, 10, 779-788.
- [13] D. Wang, Y. Zhu, C. Tian, L. Wang, W. Zhou, Y. Dong, Q. Han, Y. Liu, F. Yuan, H. Fu, *Catal. Sci. Technol.*, 2016, 6, 2403-2412.
- [14] S. Bai, L. Bu, Q. Shao, X. Zhu, X. Huang, *J. Am. Chem. Soc.*, 2018, 140, 8384-8387.
- [15] Y. Dai, X. Gao, X. Chu, C. Jiang, Y. Yao, Z. Guo, C. Zhou, C. Wang, H. Wang, Y. Yang, *J. Catal.*, 2018, 364, 192-203.
- [19] K. Yuan, T. Song, D. Wang, X. Zhang, X. Gao, Y. Zou, H. Dong, Z. Tang, W. Hu, *Angew. Chem. Int. Ed.*, 2018, 57, 5708-5713.
- [21] Y. Zhang, S. Wei, Y. Lin, G. Fan, F. Li, *ACS Omega*, 2018, 3, 12778-12787.
- [24] C. Li, C. Ke, R. Han, G. Fan, L. Yang, F. Li, *Mol. Catal.*, 2018, 455, 78-87.



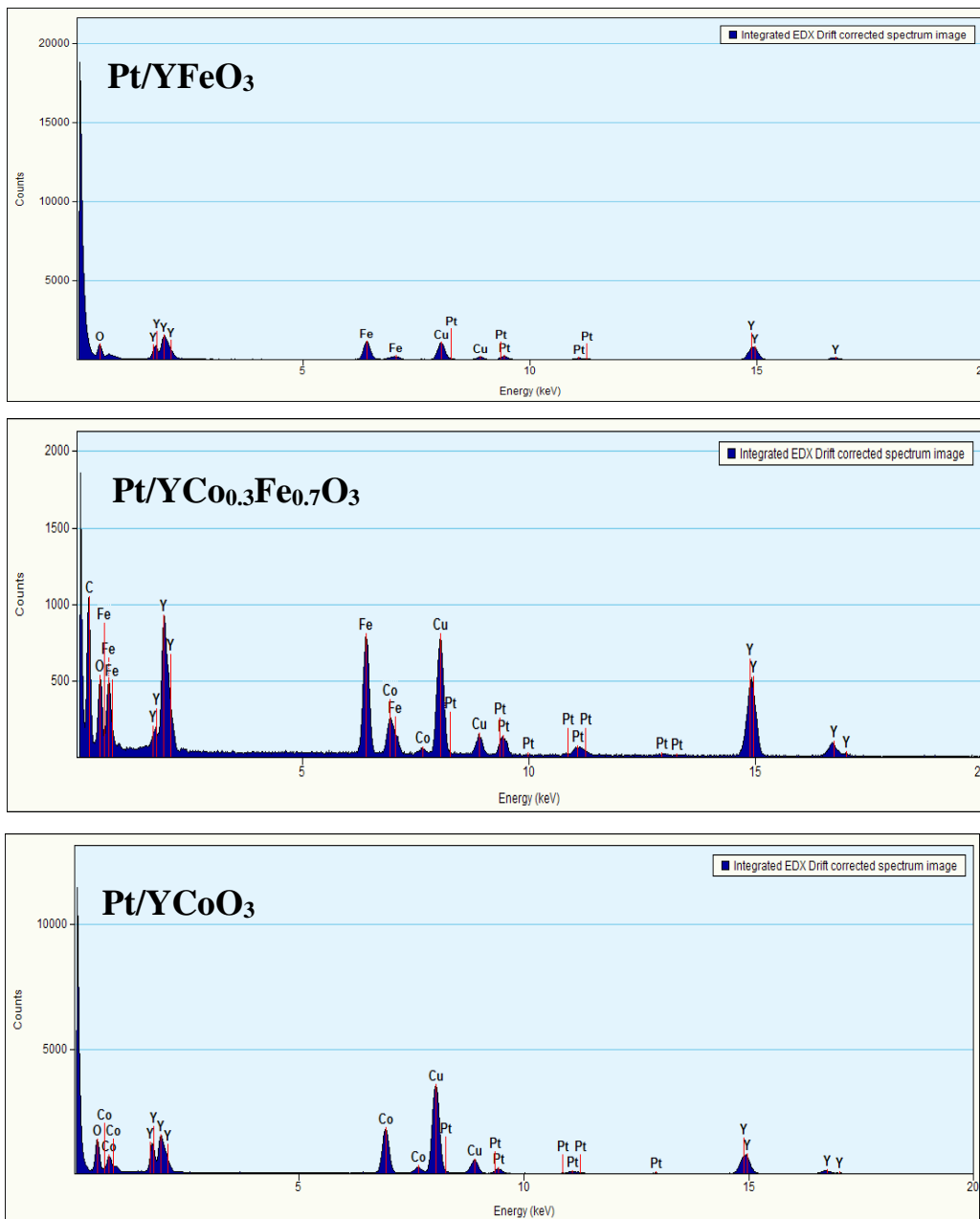


Fig. S7. HAADF-STEM images and STEM-EDS elemental mapping images for the area enclosed by the orange square for Pt/YCoO₃; Pt/YFeO₃ and Pt/YCo_{0.3}Fe_{0.7}O₃.

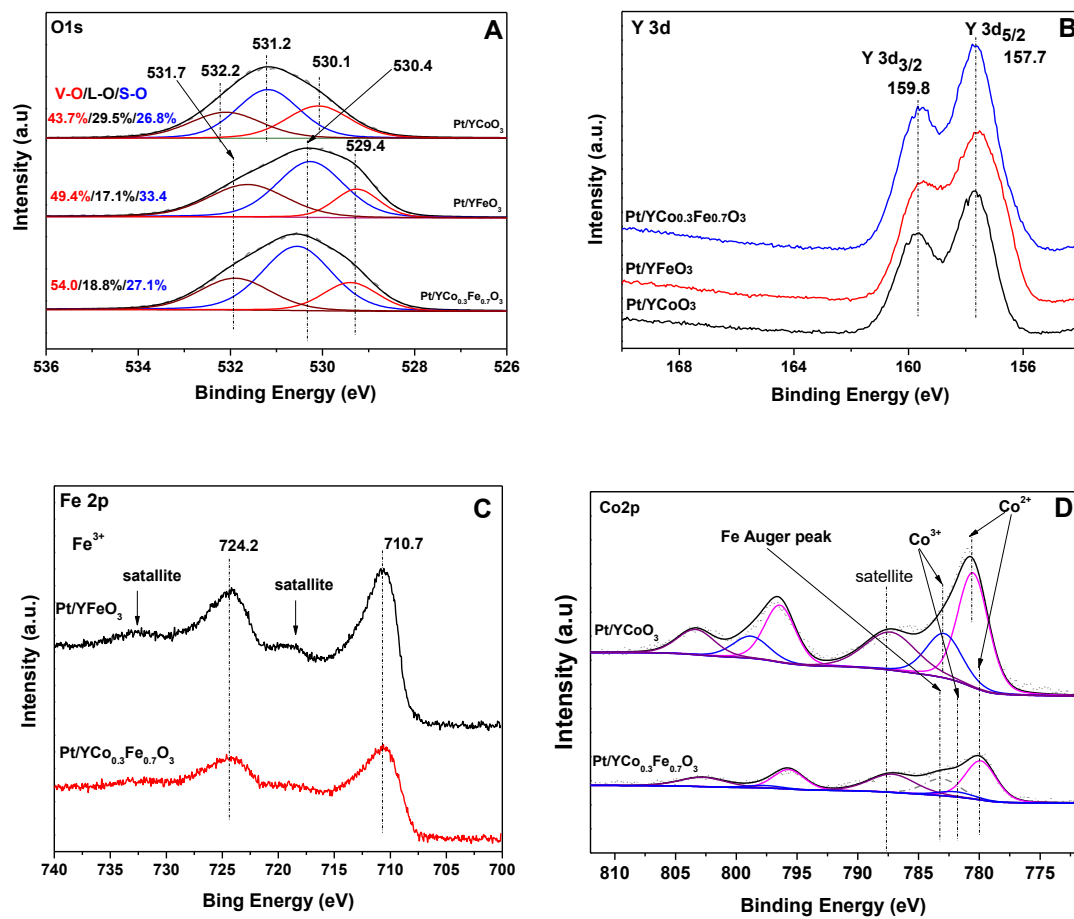


Fig. S8. XPS spectra of the Pt/YCo_xFe_{1-x}O₃ catalyst

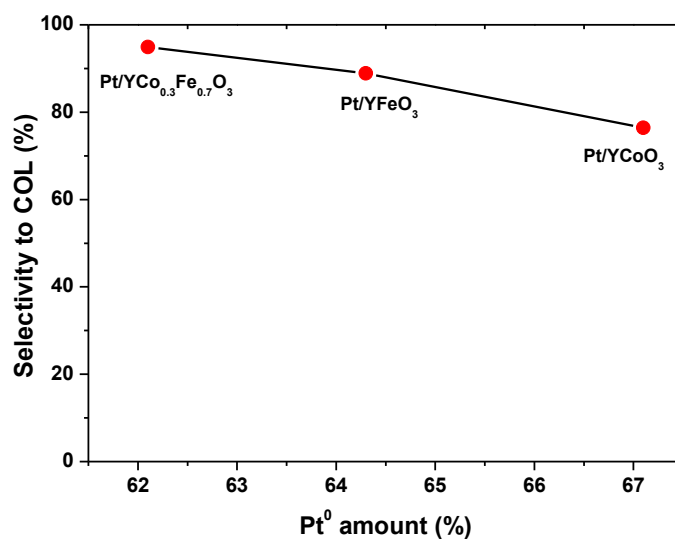


Fig. S9. The correlation of COL selectivity versus Pt⁰ amount on the Pt/YCo_xFe_{1-x}O₃ catalyst according to XPS results.